

# Material Transport in Turbulent Gas Streams: Radial Diffusion in a Circular Conduit

SCOTT LYNN, W. H. CORCORAN, and B. H. SAGE

**California Institute of Technology, Pasadena, California**

Experimental studies of the mixing of coaxial streams of a natural gas and air at atmospheric pressure were made at Reynolds numbers of 44,000 and 79,000 under conditions where the turbulent-velocity profile of nearly uniform flow was altered as little as feasible by the blending of the two streams.

Total diffusivities of natural gas in air for the region near the center of the conduit were computed from the data for turbulent, steady, nonuniform flow. The total diffusivities were found to be rather complicated functions of the conditions of flow. Limitations in the configuration of the apparatus did not permit a study of the behavior of the total diffusivities to be made over as wide a range of flow rates as would be necessary to investigate the large-scale trends indicated by this study.

The transfer processes in a turbulent stream are considered here to result from a combination of the transport associated with the molecular migration of the components of the phase and the transport due to the relative macroscopic motions resulting from turbulence in the fluid as well as its gross motion across the section. Transfer of material through a unit area of surface by diffusional processes only may be expressed for radial transport as

$$\dot{m}_{Ad} = -D_A \frac{\partial \sigma_A}{\partial r} + \overline{\sigma_A' u_r'} \quad (1)$$

where  $\dot{m}_{A_d}$  is the weight of component A transported by diffusional processes per unit area and per unit time. For convenience Equation (1) is often expressed as

$$\dot{m}_{Ad} = -(\epsilon_{DA} + D_A) \frac{\partial \sigma_A}{\partial r} \quad (2)$$

where  $\epsilon_{DA}$  is the eddy diffusivity for component  $A$ . The eddy diffusivity and molecular diffusivity, or Fick diffusion coefficient, may be combined in one term, the total diffusivity,  $\epsilon_{DA}$ . Equation (2) may then be written as

$$\dot{m}_{Ad} = -\epsilon_{DA} \frac{\partial \sigma_A}{\partial r} \quad (3)$$

Likewise equations for momentum transfer in fluid flow may be developed. The corresponding result to compare with Equation (3) for the case of a fluid flowing uniformly through a straight, circular conduit is

$$\tau = \frac{\sigma}{g} \epsilon_m \frac{\partial u_x}{\partial r} \quad (4)$$

where  $\tau$  is the shear stress in pounds per square foot. Reynolds (9) proposed that

$\epsilon_m$ , the eddy viscosity, and  $\epsilon_c$ , the eddy conductivity, were equal. Experimental evidence (11) indicates that for practical

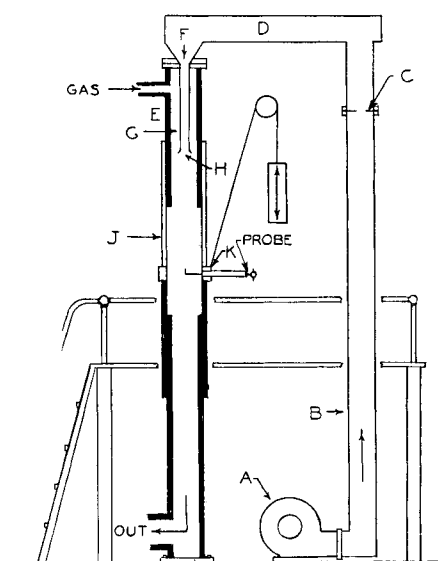


**Fig. 1. Schematic diagram of turbulent-diffusion apparatus.**

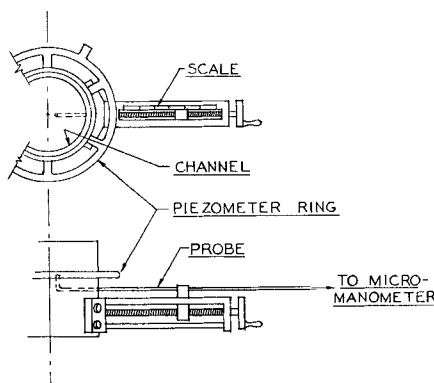


**Fig. 2. Arrangement of probe and piezometer ring.**

purposes a proportionality may be established between  $\epsilon_m$  and  $\epsilon_{D_A}$ .

It was the intent of the present work to investigate further the nature of  $\epsilon_{DA}$  in the initial mixing of two concentric streams where the turbulent-velocity profile of the central, main stream was altered as little as possible by the addition of the diffusing component. In particular it was desired to establish the behavior of  $\epsilon_{DA}$  along the axis of the coaxial streams.

## THEORY

For steady state the rate of accumulation of the diffusing component in a fixed element of volume is zero. Therefore the sum of the divergences of the convective and diffusional fluxes of the component is zero or, expressed analytically,

$$-\frac{\partial \sigma_A}{\partial t} = 0 = \nabla \cdot \sigma_A \mathbf{u} + \nabla \cdot (-\epsilon_{DA} \nabla \sigma_A) \quad (5)$$

In Equation (5) it is implicitly assumed that there is isotropic turbulence and therefore isotropic eddy diffusivity. Also the Fick diffusion coefficient is assumed to be isotropic in character. The assumptions are not necessary in the development of the final expression for the radial eddy diffusivity but are made to simplify the writing of the equations. If cylindrical symmetry is assumed and diffusional transport in the direction of flow neglected, there is obtained for a perfect gas

$$r_{\xi D_A} \frac{\partial n_A}{\partial r} = \frac{\frac{\partial}{\partial x} \int_0^r n_A u_x dr - n_A \frac{\partial}{\partial x} \int_0^r r u_x dr}{\frac{\sigma}{\sigma_{\text{max}}}} \quad (6)$$

Equation (6) is more easily used in treating experimental data if the integrations are made with respect to  $(r/r_0)^2$  where  $r_0$  is the radius of the channel. The transformation then gives for the eddy diffusivity in the  $r$  direction

$$\epsilon_{DA} = \frac{\frac{\partial}{\partial x} \left[ \left( \frac{r_0}{r} \right)^2 \int_0^{(r/r_0)^2} n_A u_x d \left( \frac{r}{r_0} \right)^2 \right] - n_A \frac{\partial}{\partial x} \left[ \left( \frac{r_0}{r} \right)^2 \int_0^{(r/r_0)^2} u_x d \left( \frac{r}{r_0} \right)^2 \right]}{\frac{4}{r_0^2} \frac{\sigma}{\sigma_{air}} \frac{\partial n_A}{\partial \left( \frac{r}{r_0} \right)^2}} \quad (7)$$

The advantages of using the variable  $(r/r_0)^2$  are twofold. Derivatives of the composition with respect to  $(r/r_0)^2$  do not go to zero at the center of the channel, and the terms being differentiated with respect to  $x$  are seen to be simply the space-average values of the respective

integrands from the center of the channel to the point in question.

An expression for the eddy viscosity may be developed also. In the analysis it is assumed that there are cylindrical

result in the following equation for steady state, turbulent flow:

$$u_x \frac{\partial \left( \frac{\sigma}{g} u_x \right)}{\partial x} = - \frac{\partial P}{\partial x} + \frac{1}{r} \frac{\partial}{\partial r} \left( r \frac{\sigma}{g} \epsilon_m \frac{\partial u_x}{\partial r} \right) \quad (8)$$

By use of the same transformation as was applied to Equation (6), the expression for the total eddy viscosity is found to be

$$\epsilon_m = \frac{gr_0^2}{4\sigma} \frac{\partial P}{\partial x} + \frac{r_0^2}{8} \frac{\frac{\partial u_x}{\partial \left( \frac{r}{r_0} \right)^2}}{\frac{\partial \left( \frac{r}{r_0} \right)^2}{\partial x}} + \frac{\partial}{\partial x} \left[ \left( \frac{r_0}{r} \right)^2 \int_0^{(r/r_0)^2} u_x^2 d \left( \frac{r}{r_0} \right)^2 \right] \quad (9)$$

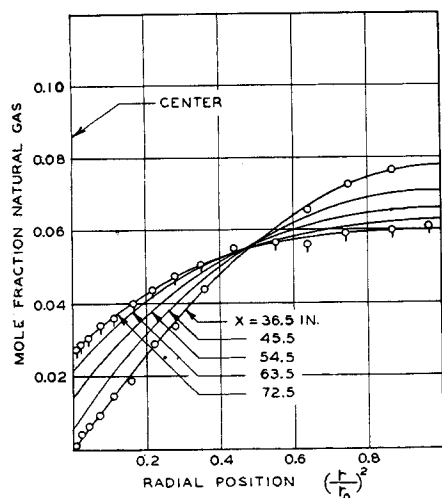


Fig. 3. Composition as a function of the square of the relative radial position—Reynolds number of 44,000.

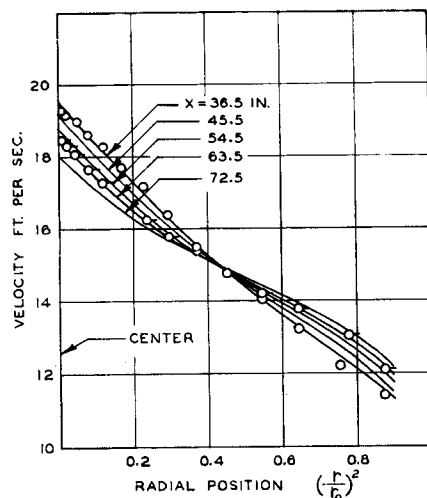


Fig. 5. Velocity as a function of the square of the relative radial position—Reynolds number of 44,000.

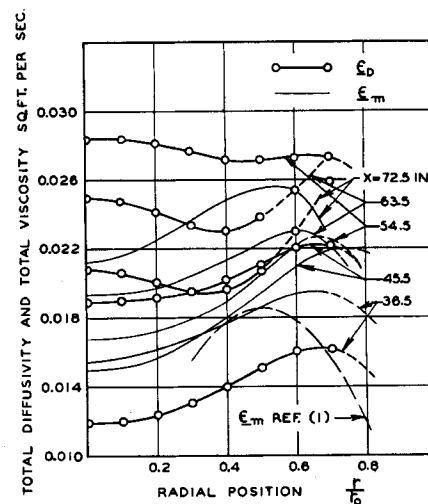


Fig. 6. Total diffusivity,  $\epsilon_D$ , and total viscosity,  $\epsilon_m$ , as functions of position—Reynolds number of 44,000.

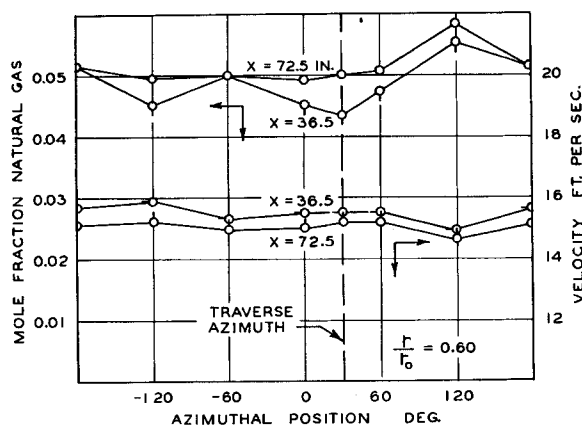


Fig. 4. Variation of velocity and composition with azimuthal position—Reynolds number of 44,000.

Since the pressure drop in gaseous streams at low Reynolds numbers is relatively small,  $\partial P/\partial x$  may be approximated from generalized friction-factor data (6) as follows:

$$-\frac{\partial P}{\partial x} = \frac{f\sigma(U_x)^2}{gr_0} \quad (10)$$

This expression neglects the effect of diffusion on the shear at the wall. The total eddy viscosity then becomes

$$\epsilon_m = \frac{-r_0^2}{4} \frac{\frac{\partial u_x}{\partial \left( \frac{r}{r_0} \right)^2}}{\frac{\partial \left( \frac{r}{r_0} \right)^2}{\partial x}} \left\{ \frac{(U_x)^2 f}{r_0} - \frac{1}{2} \cdot \frac{\partial}{\partial x} \left[ \left( \frac{r_0}{r} \right)^2 \int_0^{(r/r_0)^2} u_x^2 d \left( \frac{r}{r_0} \right)^2 \right] \right\} \quad (11)$$

In Equation (11) the second term on the

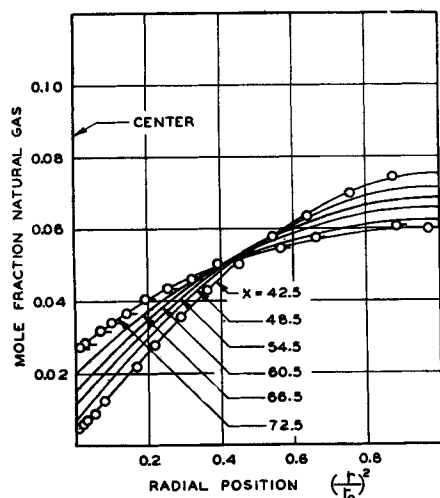


Fig. 7. Composition as a function of the square of the relative radial position—Reynolds number of 79,000.

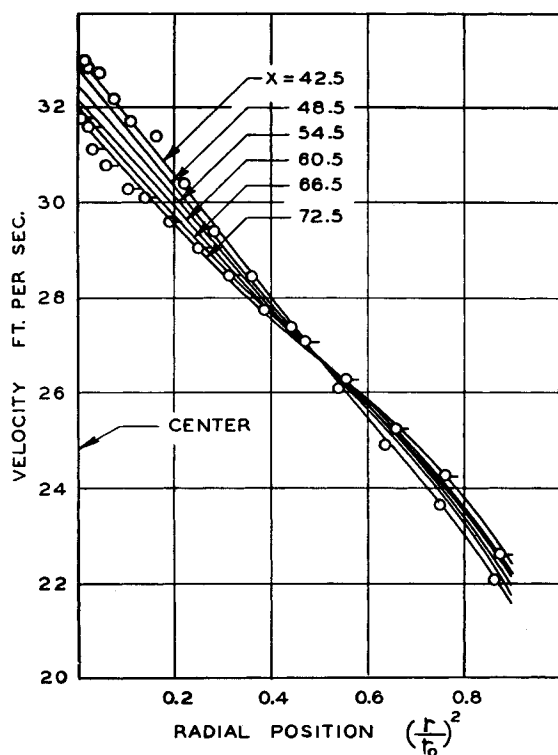


Fig. 8. Velocity as a function of the square of the relative radial position—Reynolds number of 79,000.

right-hand side is the derivative with respect to  $x$  of the space-average value of the square of the velocity from the center line to the point in question and becomes zero for uniform flow.

#### EXPERIMENTAL EQUIPMENT AND PROCEDURES

The equipment used in this study of turbulent diffusion was constructed for an earlier investigation of mass transfer between air and water droplets. Modifications were made to accommodate an annulus for the introduction of natural gas. It was realized that the upstream length from the

mixing section was not sufficient for full development of uniform flow before mixing, but the apparatus was used; nevertheless, because of interest in making at least a preliminary study of the nature of the eddy diffusivity along the center line of the flow channel.

A schematic diagram of the apparatus used in the diffusion measurements is shown in Figure 1. Air at ambient temperature was circulated by the blower *A* through a tube *B* and orifice section *C* to a plenum chamber *D* at the ceiling. Here the air changed direction and was passed down through the test section *E*, which was 6 in. in diameter. The central air stream *F* was concentric with an annulus *G* through which natural gas was introduced. Gas entered the annulus at ambient temperature and at a rate measured by a separate orifice meter. At section *H*, where the natural gas joined the central air stream, the annulus had a nominal width of  $\frac{1}{8}$  in. but a difference in radius varying between 0.120 and 0.130 in. The volumetric flow rate of the

The Lucite test section could be moved through a vertical distance of 5 ft. and rotated through an angle of 180 deg. On the test section was mounted a brass sleeve *K* holding the sampling probe with an opening 0.065 in. in diameter. The probe served also as a Pitot tube and could be moved across the diameter of the test section. At the highest traverse position the probe opening was 36.5 in. below the exit of the annulus at *H* of Figure 1. The brass sleeve *K* also served as a piezometer ring for measuring static pressures as shown in Figure 2.

The composition of the flowing stream was established by measuring the specific weight of the phase by means of a special manometer (4) with gas columns 139 in. long. The difference in weight of gas in the two columns was obtained by observing the movement of a bubble in a horizontal capillary tube connecting the two sides of the manometer (3, 7). The equation of state of a perfect gas was assumed in converting the pressure measurements to composition data.

After the velocity and composition data were obtained, they were smoothed by plotting as functions of the square of the relative radial position,  $(r/r_0)^2$ . The slopes of the curves,  $\partial u_x / \partial (r/r_0)^2$  and  $\partial n_g / \partial (r/r_0)^2$ , were smoothed with respect to  $(r/r_0)^2$  and  $x$ . The smoothed slopes were integrated to obtain the recorded values of  $n_g$  and  $u_x$ . This procedure was followed in order to increase the consistency of the results but did not decrease the uncertainty.

#### EXPERIMENTAL RESULTS

Studies of the mixing of the coaxial streams of air and natural gas were made at ambient temperature. For the first set of measurements the mean gas temperature was 71.6°F., and the bulk velocity was 14.4 ft./sec. The composition of the gas stream was 0.0435 mole fraction natural gas, taken as a mixture of methane and ethane with a mean molecular weight of 18.8, and the remainder was air. The test section had a diameter of 6 in., and the Reynolds number for the run was 44,000.

The composition measurements at a Reynolds number of 44,000 are shown in Figure 3, which also includes experimental points for  $x = 72.5$  and 36.5 in. The tabulated experimental data are available (5).

In the development of the composition data for a Reynolds number of 44,000 it was observed that the integral  $\int_0^1 n_g u_x d(r/r_0)^2$  indicated a progressive increase in the weight rate of natural gas flowing in the vertical plane common to the traverses. The apparent increase was attributed to transports in the  $\theta$  direction as a result of concentration gradients. Figure 4 shows the magnitude of the gradients. The composition and velocity data were collected in the vertical plane at  $\theta = 30^\circ$ , where the concentration gradients in the  $\theta$  direction were close to a minimum.

It was desired to compute  $\epsilon_D$  for the natural gas for the case of symmetrical

gas through the annulus was made to correspond roughly to the flow rate in the same annulus located downstream but in a full channel. Also just before reaching the  $\frac{1}{8}$ -in. annulus shown in Figure 1, the cross section of the gas stream was contracted slightly to minimize the lateral velocity component of the gas when it joined the central air stream. As the air and gas stream passed through the Lucite test section *J*, measurements of velocity and concentration were made as functions of the radius of the channel and the distance downstream from the point of initial mixing at *H*. At the outlet of the flow apparatus the mixed gases were passed through a flame holder and burned.

flow. Consequently the composition profiles obtained experimentally were corrected. A reasonable basis for such corrections appeared to be an approach leaving the shape of the profiles unchanged as well as the concentration at the center of the channel. The experimental composition profiles were adjusted to follow the equation of continuity for the hydrocarbon constituent by equating the average concentration at each traverse to that at  $x = 54.5$  in. The magnitude of the corrections to  $n_g$  did not exceed 7% of the local value.

Besides the corrections to  $n_g$  described it was also necessary to adjust the velocity 0.2 ft./sec. or about 1% of the center-line velocity at a downstream distance of  $x = 72.5$  in. and a Reynolds number of 44,000 in order to satisfy the equation of continuity for the stream as a whole. The velocity data are shown in Figure 5.

From the symmetrical velocity and composition data, values of  $\epsilon_D$  and  $\epsilon_m$  were computed by use of Equations (7) and (11) respectively. Figure 6 shows the results. There is also included in Figure 6 a curve showing  $\epsilon_m$  as obtained (1) for steady, uniform flow between parallel plates.

Another set of measurements was made at a Reynolds number of 79,000, which corresponded to a bulk velocity of 26.4 ft./sec. The mean temperature was 75.2°F. and the composition of the exit stream was 0.0481 mole fraction natural gas.

Smoothed composition data are shown in Figure 7 and Table 1. Figure 8 records the corresponding velocity data. As in the case of the lower Reynolds number, corrections were made to  $n_g$  in order to compute  $\epsilon_D$  for symmetrical flow. Figure 9 depicts the variation of velocity and composition with azimuthal position. Figure 10 shows values of  $\epsilon_D$  and  $\epsilon_m$  for the Reynolds number of 79,000. Also shown in Figure 10 is a plot of  $\epsilon_m$  as obtained for steady, uniform flow between parallel plates (1).

Random fluctuations in the compositions and velocities at a Reynolds number of 79,000 were initially much greater than for the measurements at the lower Reynolds number. To mitigate the condition a grid with triangular holes 0.25 in. on a side constructed from wires 0.1 in. in diameter was placed in the air channel 4.0 ft. above the exit of the annulus. The large-scale fluctuations were substantially reduced. The mean values of the point compositions were, however, essentially unchanged. Also the effect of the grid on the smaller scale turbulence in the stream should have been in a large measure damped out by the time an element of fluid reached the point of the discharge of the annulus (2).

It was observed that the axes of symmetry of the velocity and composition profiles did not correspond to the axis of the channel as they did at the lower

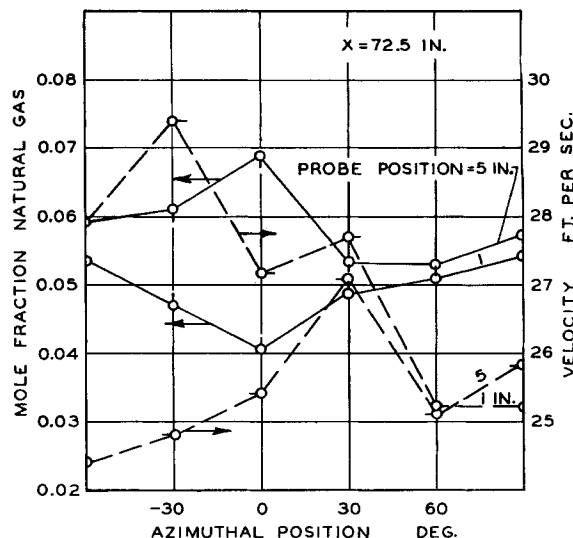


Fig. 9. Variation of velocity and composition with the azimuthal position—Reynolds number of 79,000.

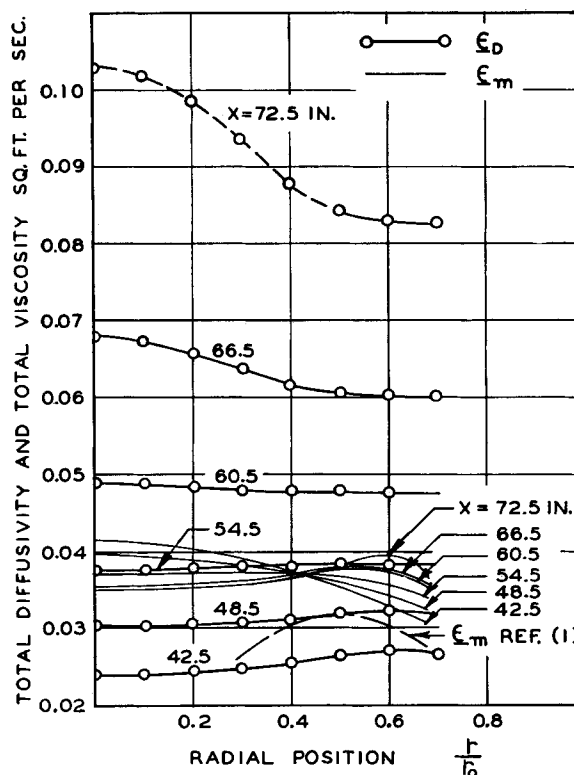


Fig. 10. Total diffusivity,  $\epsilon_D$ , and total viscosity,  $\epsilon_m$ , as functions of position—Reynolds number of 79,000.

Reynolds number. As the downstream distance increased, the displacement became greater. At  $x = 72.5$  in. the displacement was approximately 0.2 in. The warping of the concentration and velocity profiles was thought to result primarily from eccentricity in both the annulus and the Lucite tube. The maximum variation from the nominal inside diameter of 6 in. for the Lucite tube was 0.03 in.

As a check on the slightly nonuniform flow when diffusion was occurring, velocity profiles were obtained for the case where no natural gas was flowing through the system. Figure 11 shows the results for the case where the total flow rate was approximately the same as for the diffusion experiment at a Reynolds number of 44,000. It can be seen that the nonuniformity was associated with the geometry of the channel and was not

a result of diffusion. The dashed lines represent the regions of greatest uncertainty in the measurements

## DISCUSSION OF RESULTS

The Fick diffusion coefficient  $D$  for methane in air at 32°F. is  $1.7 \times 10^{-4}$  sq. ft./sec. (10) and the kinematic viscosity for air at 70°F. is  $1.64 \times 10^{-4}$  sq. ft./sec. (8). By comparison of these molecular quantities with the eddy quantities in Figures 6 and 10, the large contribution of turbulent exchange to material and momentum transfer may be observed.

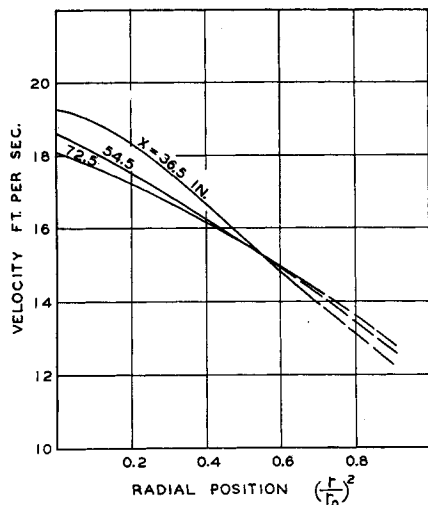


Fig. 11. Change of velocity with distance downstream in absence of diffusion—Reynolds number of 44,000.

Uncertainties in the values of  $\epsilon_D$  for the particular experimental arrangement stem mainly from the effects of the slight eccentricities in the annulus section and the Lucite tube combined with an insufficient length of straight section before the mixing of the coaxial streams of air and natural gas. The short length of straight section did not allow satisfactory development of normal uniform flow in the central air stream, as the approach was only 8 diameters in length as compared with a recommended value of 45 diameters (12). As a result of the channel geometry there was a  $\theta$  or azimuthal component of velocity as well as components in the  $r$  and  $x$  directions. The flow was not then just two-dimensional in the  $r$  and  $x$  directions. Even though suitable corrections were made for the lack of symmetry, use of a channel allowing strictly two-dimensional cylindrical flow would greatly improve the analysis of the results.

The values of the eddy diffusivity calculated from Equation (7) are sensitive to the change in composition with respect to distance along the flow channel. Eddy diffusivities in the present work are least reliable at the upper and lower ends of

the working section, as at these locations greater corrections were made in the measured composition of the stream. The values of the eddy diffusivity are not believed to involve probable errors greater than 15% for the conditions studied.

In the case of the eddy viscosity, part of the uncertainty arose from the fluctuations in the velocity data. The corrections to composition had no effect on the values of eddy viscosities. Since the pressure drop was not well defined, the error introduced by using data obtained from correlations for pipes has a direct influence on the eddy viscosities, as may be seen from Equation (9). It is estimated, however, that the eddy viscosities do not involve probable errors greater than 15%.

Both the eddy diffusivity and eddy viscosity are most reliable for values of  $(r/r_0)$  between 0.3 and 0.6, less reliable near the center of the channel, and least reliable at the walls. The regions of greatest uncertainty are indicated by the dashed curves. The gradation in uncertainty is partly the result of the corrections to the composition profiles and partly a natural consequence of the mathematical treatment of the terms in the equations for the eddy quantities.

## CONCLUSIONS

From the consideration of composition and velocity as functions of  $(r/r_0)^2$ , values of the eddy diffusivity and the eddy viscosity may be established for the central portion of a nearly symmetrically flowing stream. Use of  $(r/r_0)$  as the independent variable does not permit direct ascertaining of the center-line values of the eddy properties.

The eddy properties are complicated functions of the particular conditions of flow and channel geometry. In particular, the eddy diffusivity is especially sensitive because of the association between mass transfer of a particular component and momentum transfer. When values of the eddy diffusivity are reported, they should be defined in terms of the particular transfer and channel conditions.

## NOTATION

$A_A$	= Fick diffusion coefficient for component A, sq. ft./sec.
$d$	= differential operator
$f$	= Fanning friction factor
$g$	= gravitational constant, 32.2 ft./sec. <sup>2</sup>
$\dot{m}_{A_A}$	= weight rate of component A transport by diffusional process, lb./(sq. ft.)(sec.)
$n_A$	= mole fraction of component A
$n_g$	= mole fraction natural gas
$P$	= pressure, lb./sq. ft.
$r$	= radial coordinate in the system of cylindrical coordinates, ft.
$r_0$	= radius of channel, ft.

$t$	= time, sec.
$\mathbf{u}$	= vector velocity
$u_r'$	= fluctuating component of radial velocity, $u_r$ , ft./sec.
$u_x$	= time-average point velocity in $x$ direction, ft./sec.
$U_x$	= bulk velocity, ft./sec.
$x$	= axial coordinate in the system of cylindrical coordinates, ft.
$\nabla$	= del, a vector operator
$\epsilon_0$	= eddy conductivity, sq. ft./sec.
$\epsilon_D$	= total diffusivity for natural gas, sq. ft./sec.
$\epsilon_{D_A}$	= eddy diffusivity for component A, sq. ft./sec.
$\epsilon_{D_A}$	= total diffusivity for component A, sq. ft./sec.
$\epsilon_m$	= eddy viscosity, sq. ft./sec.
$\epsilon_m$	= total viscosity, sq. ft./sec.
$\theta$	= angular coordinate in the system of cylindrical coordinates, radians
$\sigma$	= specific weight of system, lb./cu. ft.
$\sigma_A$	= time-average point concentration of A, lb./cu. ft.
$\sigma_A'$	= fluctuating component of concentration of A, lb./cu. ft.
$\overline{\sigma_A' u_r'}$	= time average of indicated product, lb./(sq. ft.)(sec.)
$\sigma_{air}^0$	= specific weight of air at temperature and pressure for a given point, lb./cu. ft.
$\tau$	= shear stress in $x$ direction, lb./sq. ft.
$\partial$	= partial-differential operator

## LITERATURE CITED

- Connell, W. R., W. G. Schlenger, and B. H. Sage, Document 3657 Am. Doc. Inst., Library of Congress, Washington, D. C. (1952). Price: \$1.00 for photoprint or \$4.65 for 35-mm. microfilm.
- Davis, Leo, Report 3-17, Jet Propulsion Laboratory, Calif. Inst. Technol. (1952).
- Henry, A., *Compt. Rend.*, 155, 1078 (1912).
- Lynn, Scott, W. H. Corcoran, and B. H. Sage, *Rev. Sci. Instr.*, 27, 368 (1956).
- Lynn, Scott, W. H. Corcoran, and B. H. Sage, Document 5122. Am. Doc. Inst., Library of Congress, Washington, D. C. (1957). Price: \$2.50 for photoprints or \$1.75 for 35-mm. microfilm.
- McAdams, W. H., "Heat Transmission," McGraw-Hill Book Company, Inc., New York (1954).
- Ower, E., *Reports & Mem. No. 1308*, Aeronaut. Research Comm., Gr. Brit. (1930).
- Page, Franklin, Jr., W. H. Corcoran, W. G. Schlenger, and B. H. Sage, *Ind. Eng. Chem.*, 44, 419 (1952).
- Reynolds, O., *Proc. Manchester Lit. Phil. Soc.*, 14, 7 (1874).
- Sherwood, T. K., and R. L. Pigford, "Absorption and Extraction," McGraw-Hill Book Company, Inc., New York (1952).
- Sherwood, T. K., and B. B. Woertz, *Trans. Am. Inst. Chem. Engrs.*, 35, 517 (1939).
- Towle, W. L., T. K. Sherwood, and L. A. Seder, *Ind. Eng. Chem.*, 31, 462 (1939).